BNL 9911
Conf - 754-6

6th IBM Medical Symposium

Poughkeepsie and
Brookhaven National Laboratory

October 5-9, 1964

POSITRON SCANNER FOR BRAIN TUMORS *

J.S. Robertson, M.D., Ph.D. and S.R. Bozzo, M.D.
Brookhaven National Laboratory

1. INTRODUCTION

For some time we have had under development a multi-detector positron scanner for use in locating brain tumors. A previous progress report was presented at the 1962 IBM Medical Symposium (1), and the basic device has been described by Rankowitz et al. (2).

Briefly, the principle of the device is as follows. In the annihilation of a positron, or β^+, two gamma rays, each of 0.511 MeV, are emitted in opposite directions. Such an event may be detected with two gamma-ray counters connected in a coincidence circuit. Since there are positron-emitting substances that tend to localize preferentially in brain tumors (3, 4), this method can be, and is being, used to locate brain tumors. However, scanning with only two detectors takes about 40 minutes time, and at least two such scans are needed for three-dimensional localization. It was thought that if a multi-detector device could be developed, the scanning time would be greatly shortened, with such consequent advantages as being able to work with lower doses of radiation, to obtain serial determinations, and to work with shorter-lived isotopes.

It was originally thought that a three-dimensional distribution of the detectors could be used, giving a complete picture of the distribution of positron activity in a single set of counts. However, the mathematical difficulties encountered in resolving the data generated by such an array led to a partial compromise in which 32 one-inch diameter NaI crystals are arranged in a ring, as shown in Slide 1. This device therefore sees only a laminographic-type section of the head about 2 cm thick, and several sets of counts are needed to scan the entire head. Even so, the procedure is much shorter than when only two detectors are used.

2. Mathematical Considerations

The data obtained with any given pair of detectors are the sum of all of the counts that originate in the volume "seen" by that pair, modified by the geometry factor and other factors that affect the crystal's efficiency. (Slides 2 and 3.) At the time of the previous report (1), it had been hoped

* Research supported by the U. S. Atomic Energy Commission.

DISCLAIMER

that information giving the distribution of activity could be obtained by solving a system of simultaneous equations, with the volume of interest divided into the same number of elements of volume as the number of useful counter pairs. The simultaneous equations method proved to be impracticable, however, and other approaches were tried. Of the several other approaches, only the one developed by Dr. Bozzo has been tested clinically and it will be emphasized here. This method is described as follows:

In order to analyze the data, a mathematical model is developed, upon which the computer program for solution and for display of the results is based.

The model will involve only a plane of interest, the limits of which will be the circle defined by the detector array.

Within this plane any point can be represented by an expression Ac(i, j) where Ac is the activity at the point i, j.

The total activity within the plane will be

$$\text{Total Activity} = \sum_{i}^{n} \sum_{j}^{\rho} Ac(i,j)$$

Where n and ρ represent the upper limits of the area under consideration expressed in the incremental units L for n, and m for ρ.

The complete distribution of activity in the plane can be represented in general form by the matrix

$$\begin{bmatrix} Ac(L,m) & & \\ & \ddots & \\ & & Ac(n,\rho) \end{bmatrix}$$

In order to choose appropriate values for the limits n and ρ, as well as the practical values for L and M, we study the different sectors defined by various pairs of counters.

In Slide 4 we can see different sectors defined by randomly chosen pairs.

If we impose some conditions on the pair ordering such as a particular number of detectors apart, then we obtain several sets of counter pairs with some particular sector defined by each set.

Slide 5 illustrates some of the sectors generated by considering different sets.

By generalizing this condition, we can obtain 16 unique sets of pairs, each one defining a particular sector of the plane in our model. This general condition can be expressed by:

$$N = M + 1 \longrightarrow N = M + 16$$

where M is any detector subscript (1---32)
and N is any coincident detector subscript (1---32)

The different sectors defined by the 16 sets are 15 concentric rings and a circle with zero radius at the center of our model.

In order to obtain a further division in the individual rings, we now analyze how a particular sector of a given ring is represented in a set of pairs.

As we can see in Figure 6, the condition

$P(N, N+9) \cong P(N+1, N+10)$ where $P(n, m)$ represents the counts in the pair (n, m) is only satisfied by a single source if it is located in a particular ring and within this ring in a particular sector.

From here we can derive the necessary conditions that will allow us to represent locations of sources at 32 points within each ring. Also from the preceding considerations we can derive two constants in our system:

a) that the data contain at least 16 sets of counter pairs, each one related to a particular sector of the plane,

b) that each set contains 32 elements, each one related to a particular sector within a ring.

Furthermore, the relation between the sectors defined by the different sets is an additive one.

It is convenient to rearrange the data matrix by a transposition of the elements from:

$$\begin{bmatrix} D(1,1) & & & \\ & \ddots & & \\ & & & D(32,32) \end{bmatrix}$$

to:

$$\begin{bmatrix} D(1,2) & & & \\ & \ddots & & \\ & & & D(n,m) \end{bmatrix}$$

where $n = 1 --- 32$
and $m = n + k$
with $k = 1 --- 16$

The data matrix will contain some particular properties that will be useful in the reduction and solution for unknown distributions.

a) The different columns will contain data related to particular concentrics circles of the plane. A special case will be the one where the location of the source is in the center of the plane. The following results (Slides 6, 7, 8) show the relation between predicted and actual data in such a case.

Since the sectors formed by the counter pairs represented by the equations

$$M = 1, 32 \quad - \quad \begin{Bmatrix} N = M + 1 \\ \cdot \quad \cdot \quad \cdot \\ \cdot \quad \cdot \quad \cdot \\ N = M + 4 \end{Bmatrix}$$

do not actually cover the model as seen in Slide 9, we can reduce the data matrix to one of order 32 x 12.

The data observed by the detectors represent some distribution of activity within the model after undergoing a linear transformation by the matrix T.

$$D = T.A.$$

Furthermore, the observed data can be represented as a linear combination of known libraries.

$$\left| \text{Data } m,n \right| = \sum_{n=1}^{12} \sum_{m=1}^{32} \left[\lambda_{m,n} \left| L_{m,n} \right| \right]$$

where $L_{m,n}$ is the matrix representing the efficiency factors of the detectors with respect to the coordinate position (m, n) in the model.

The $\lambda(m,n)$ values are the multiplicative constants associated with the various libraries which are found to be contained in the data $\lambda(m,n)$ times.

The fitting algorithm searches for the λ values until the following condition is met.

$$\left| D_{ij} \right| - \left[\sum_{j=1}^{12} \sum_{i=1}^{32} \lambda_{ij} \left| L_{ij} \right| \right] < \epsilon \text{ for all i and j.}$$

The resulting matrix $\left| \lambda_{ij} \right|$ then represents an activity matrix which is related to the initial distribution within the model.

$$\left| \lambda_{i,j} \right| \sim \left| ACT_{i,j} \right|$$

3. General Procedure

The numerical output from the scanning device is on paper tape and these data after a straight conversion to magnetic tape are input to the CHEAD program. The data are in a form in which the counts detected by each of the 1,024 possible counter pairs are expressed uniquely. The counts in any given (i, j) pair of detectors are directly related to the activity within the volume subtended by the pair as well as any random coincidence counts.

Use is made of a master library which contains individual distributions for 384 symmetrically-distributed point sources across a horizontal cut of a model head.

Since the physical radius of the scanning device is larger than the average head, a finite volume which is relatively free of any concentrated activity is introduced, a covering of which is obtained by considering those counters which are five or less apart. Thus the counts observed by counter pairs defined by the egs. M = 1, 32, N = M + 1, . . . , M = 1, 32, N = M + 4 can be ignored since they are not related to any real distribution of activity, but not those starting with M = 1, 32, N = M + 5 which view defined volumes of the head. (See Figure 7.)

With this in mind, we generated a library of 384 distinct distributions.

Each of the library matrices is of order 32 x 12 where position (1, 1) represents the activity as seen by counters (1, 6) and position (32, 1) the activity seen by counters (32, 5). Column two represents the activity seen by counters (1, 7), (2, 8) ... (32, 6). Column twelve represents (1, 17), (2, 18) ... (32, 16).

The data are ordered in the same way as the library matrices are after suitable editing and correcting for the relative efficiency of each counter. The relative efficiencies are derived from the actual counts observed from a source point placed at position (0, 0). This procedure is applied daily prior to the actual scanning for that day. At this point the fitting algorithm is applied. It proceeds from the outlying region of the head and works toward the center. The highest activity in the first column is noted in the data, and a comparison between the data and the library associated with that (i, j) position in the data matrix is made. The smallest non-zero element and its (i, j) position after a one-to-one ratio has been found are set aside in the (i, j)th position of a multiplication matrix. This procedure is repeated until the entire column has been processed. The activity matrix at this point represents the distribution of sources in the outermost disc of the model.

Each distribution is the result of considering a uniform point source at a particular (i, j) position within the model. Then 384 (i, j) points are the midpoints of the lines joining the counter pairs M = 1, 32, N = M + 5, M = 1, 32 ... N = M + 16.

The source points so chosen were decided upon, since they afforded a symmetric distribution with a heavy concentration as the center was approached.

The probability, as a function of the angle, of a given source point being seen by the various counter pairs, yields the distribution for a given point. This is done for all 384 points. Thus a given library matrix represents a distribution which would, after a suitable normalization, result if a uniform source of activity were placed at the given (x, y) coordinate in the model. Since we are dealing with the positron annihilation, we expect gamma rays equal in intensity but opposite in direction to result. Thus we expect that, for a source at the center of our model, the probability of detection by counters (1, 6) to be zero, while equal to one for the pairs (1, 17), (2, 18), etc. With actual data there are always residual data that are related to random distributions of counts, and possibly contains some information about sources not covered by our library.

The procedure is then applied to the remaining 11 columns. After the subtractions are completed, the multiplicative matrix contains the multipliers of each of the subtracted libraries that are contained in the initial data. Since the initial libraries were generated by considering the effects of uniform point sources, our activity matrix represents the input data in terms of known point sources and their constant multipliers.

4. Clinical Results

In cooperation with Dr. W. Sweet and Dr. S. Aronow at the Massachusetts General Hospital in Boston, a series of patients with symptoms of intracranial lesions were scanned both by the standard two-detector method and with the multi-detector scanner.

A comparison of the results obtained with the two methods in three representative patients is shown in Figures 4, 5, and 6. The conventional scans are shown in the upper halves of Figures 4 and 5, and on the left in Figure 6. The multi-detector results depict the distribution of activity in the planes indicated by letter pairs (A, A') in the conventional scans. The subscripts indicate the relative orientations. The height of the pyramids is proportional to the concentration of activity above the cut-off level at the location of the base of the pyramid.

Figure 4 shows the results obtained by both methods in a normal subject. The peaks that occur are attributed to concentration of activity in muscle masses of the head.

Figure 5 is of a patient with a tumor in the right frontal lobe. Here the pyramids are clearly well within the skull and the sharpest localization appears in the B and C planes. The scattering of pyramids in the A plane indicates a more homogeneous distribution.

In Figure 6 a tumor in the right patietal lobe is clearly shown in the conventional scan. The two planes scanned by the multi-detector method bracket the affected volume, but the localization is indicated in the A plane.

Discussion

The figures shown of the clinical results are an attempt to translate the mathematically-derived results into a display that is immediately meaningful to the surgeon. In this process all values more than a selected ratio below the peak value are suppressed. Further work is needed to determine the optimal cut-off, and other forms of display are being considered. In any event, the actual numerical values are available for comparison.

Another somewhat different mathematical approach has been developed by J.D. Pincus (5) and programmed by N. Reese of the B.N.L. Applied Mathematics Division. This program was not available in time for processing the clinical data reported here, so results with it cannot be discussed. The method may, however, be described very briefly as follows. A given chord (i, j) connecting two counters, i and j, is characterized by a unit normal vector, X (θ), and a (signed) distance, ρ, from the center. The viewpoint is adopted that the actually observed counts C (i, j) are a sampling of a continuous count function C (ρ, θ). A Fourier series is used in an interpolation procedure to construct the required continuous function. A final integration provides the basis for calculation of a field of weighted lattice points which may be displayed numerically or as intensity variations on an oscillographic screen.

REFERENCES

1. J.S. Robertson and A.M. Neill, Use of a Digital Computer in the Development of a Positron Scanning Procedure, Fourth Medical Symposium, IBM, October 22-26, 1962, Endicott, New York.
2. S. Rankowitz, J.S. Robertson, W.A. Higinbotham, and M.J. Rosenblum, IRE International Convention Record, Part 9, pp. 49-56, 1962.
3. W.H. Sweet and G.L. Brownell, Localization of Intracranial Lesion by Scanning with Positron-Emitting Arsenic, JAMA, 157, 1183, 1955.
4. H.J. Bagnall, P. Benda, G.L. Brownell, and W.H. Sweet, Positron Scanning with Copper-64 in the Diagnosis of Intracranial Lesions. J. Neurosurgery 15, 411-426, 1958.
5. J.D. Pincus, A Mathematical Reconstruction of a Radioactive Source Density from its Induced Radiation Pattern. To be published.

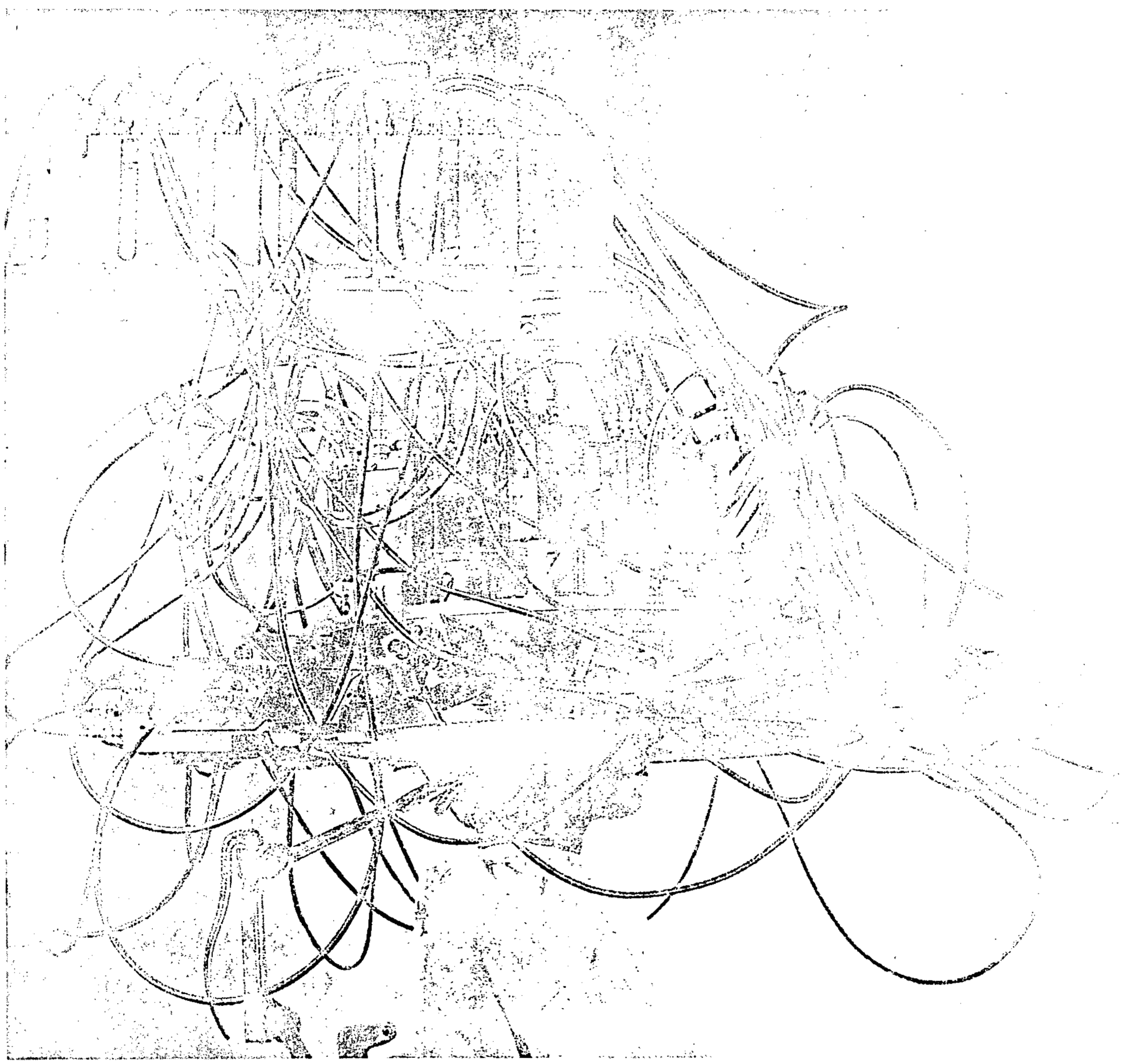

Figure 1: Multi-detector positron scanner as used for locating brain tumors. The 32 NaI crystals are in one plane, but the photomultiplier tube assemblies are alternately horizontal and vertical to permit close packing.

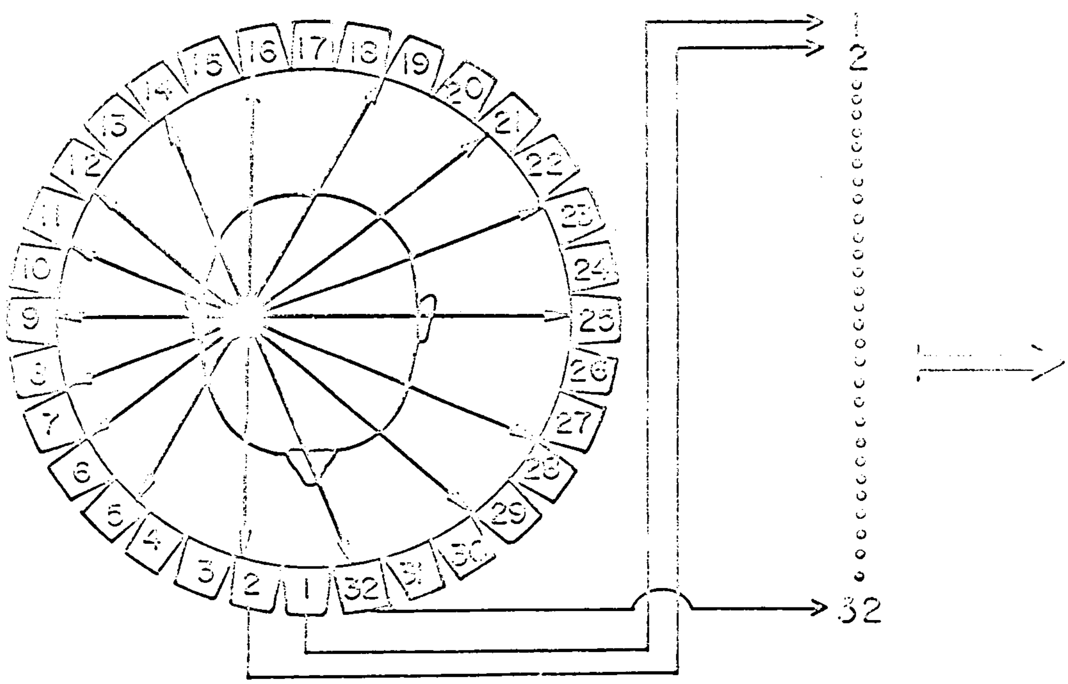

3 γ RAYS FROM ANNIHILATION GENERATE PULSES IN A 32 DETECTOR ARRAY

Figure 2: Schematic relationship between brain tumor, detector array, and coincidence recording equipment.

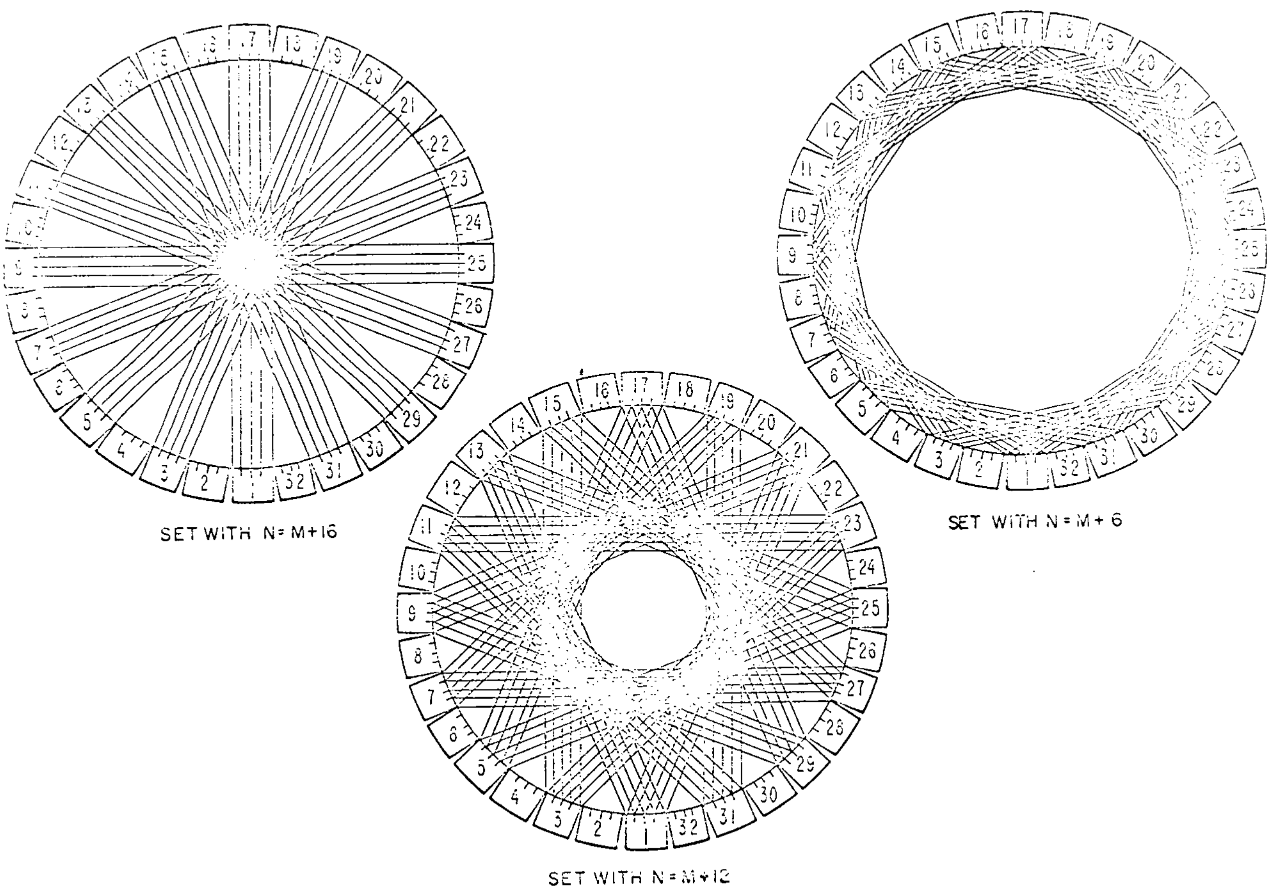

Figure 3: Zones of activity "seen" by different sets of detector pairings. The notation N = M + A indicates that in the designated set the number of the second member of a pair is A greater than that of the first, modulo 32.

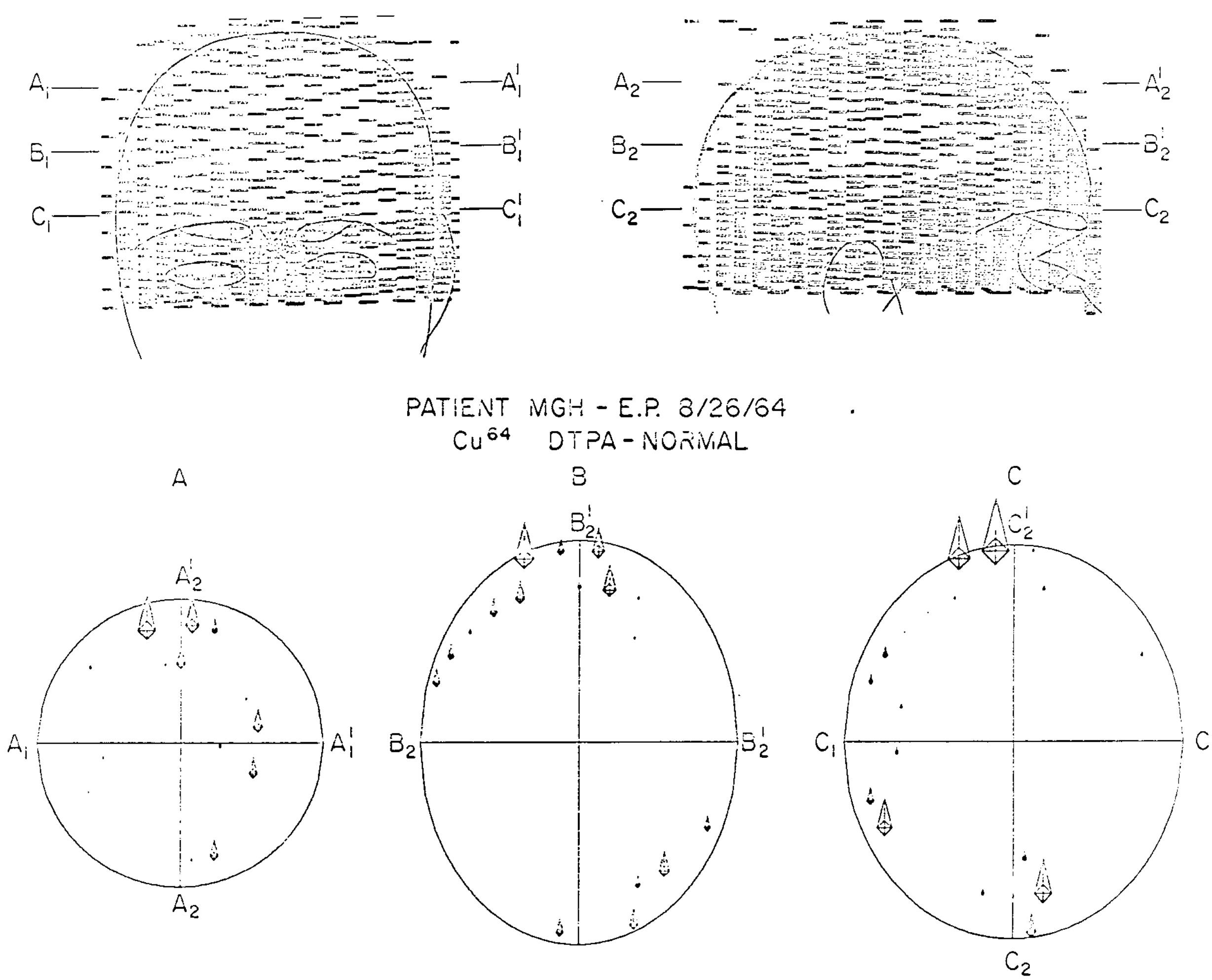

Figure 4: Scans taken after injection of Cu^{64} DTPA in a normal subject. Neither the conventional scans (upper) nor the multi-detector scans (lower) show abnormalities of isotope distribution, or significant local concentrations. See text for explanation of of symbols used in multi-detector scan and for relationships among the scans.

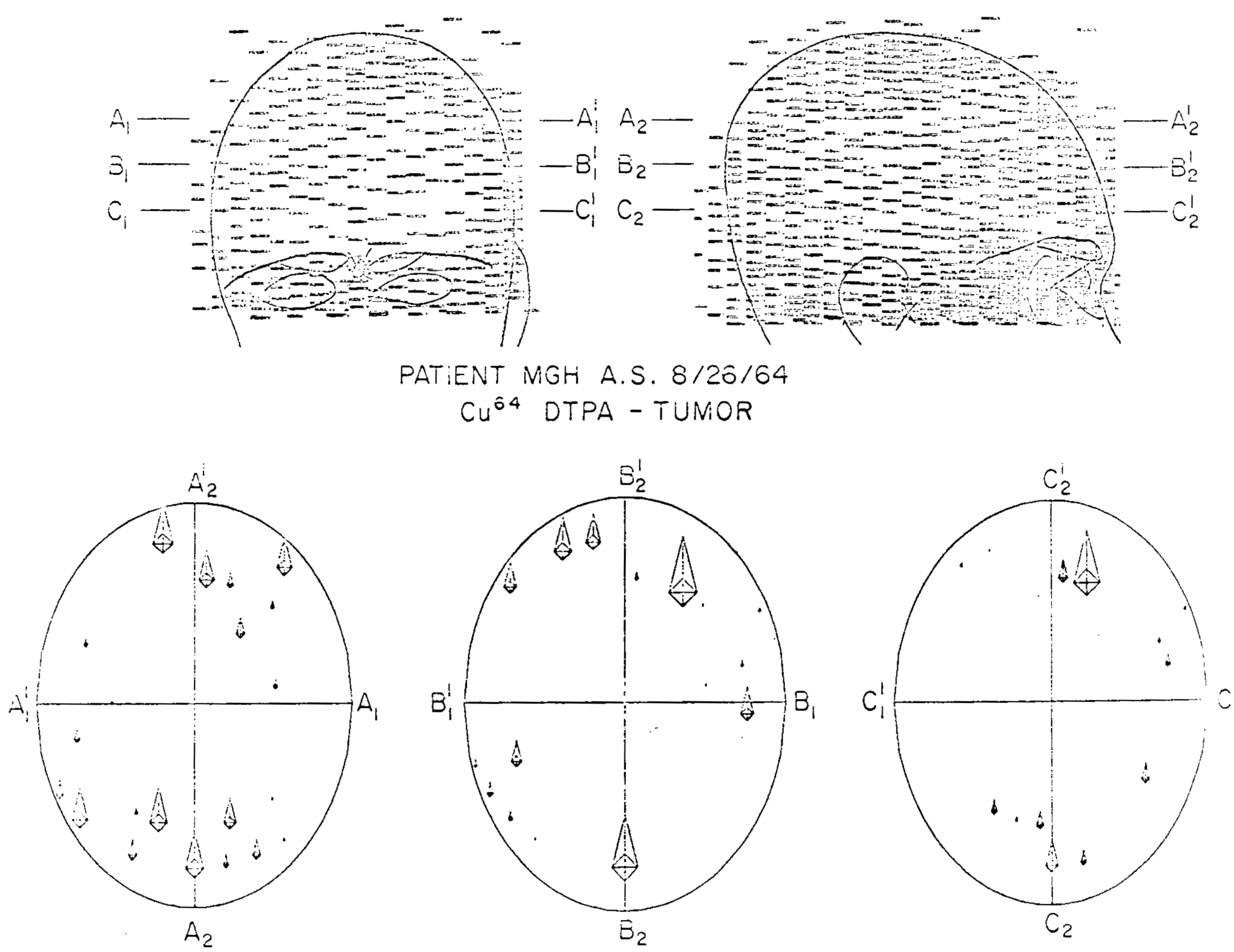

Figure 5: Scans taken after injection of Cu^{64} DTPA in a patient with a frontal lobe tumor. The conventional scans were taken 1 hour after injection; the multi-detector ones 24 hours later.

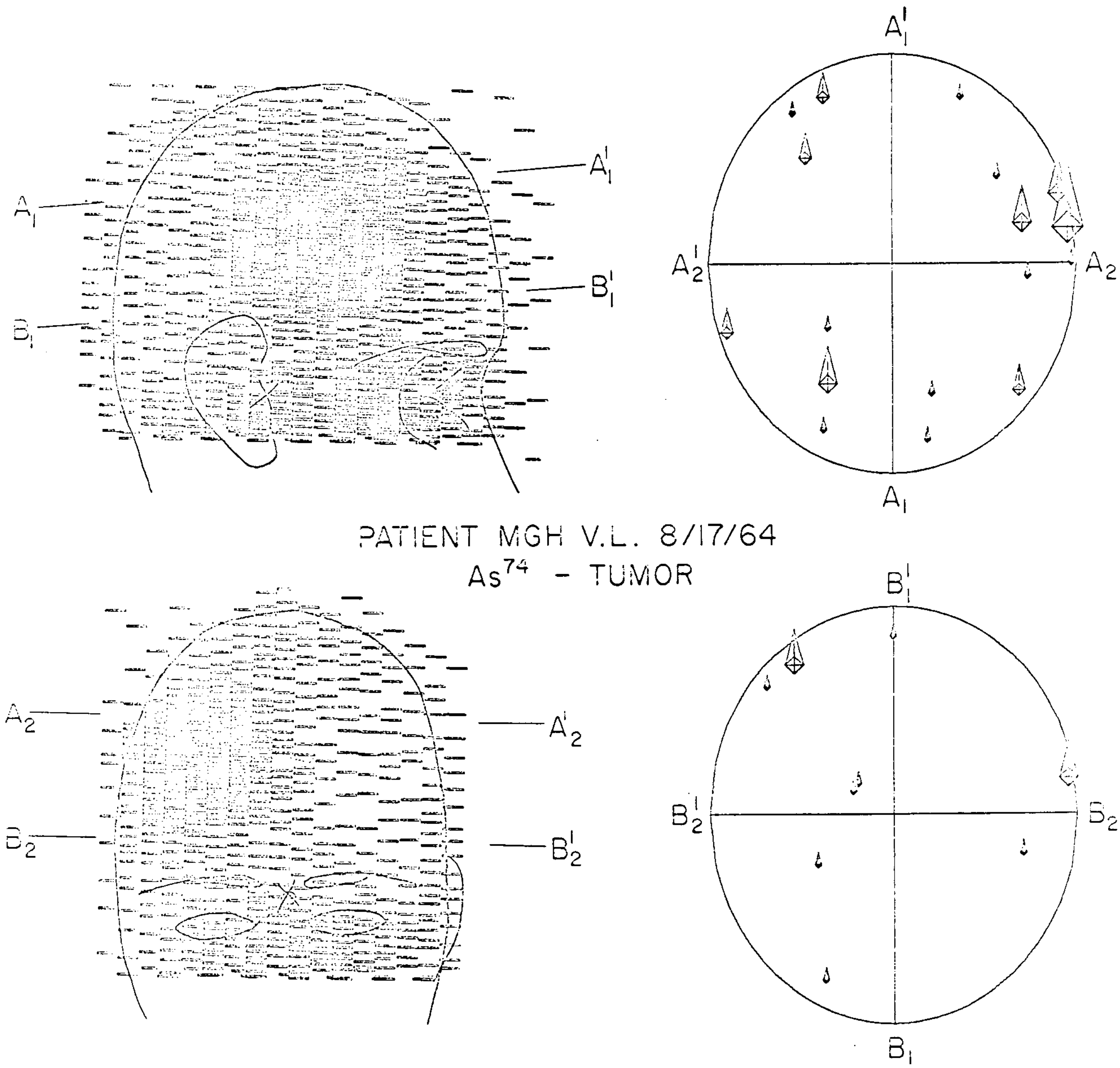

Figure 6: Scans taken after injection of As^{74} in patient with a tumor in the right parietal lobe. (1 hour afterwards for conventional, left, and 24 hours afterwards for multi-detector, right.) Multi-detector laminal bracket the tumor, but localization is shown in the "A" section.